Int. J. Electrochem. Sci., 9 **(2014)** 4217 - 4229

International Journal of
ELECTROCHEMICAL
SCIENCE
www.electrochemsci.org

Corrosion Characterisation and Passivation Behavior of $Fe_{68.6}Ni_{28.2}Mn_{3.2}$ Alloy in Acidic Solution

Khadijah M. Emran

Chemistry Department, College of Science, Taibaj University, Al-Madinah Al-Monawarah, Kingdom of Saudi Arabia.
*E-mail: kabdalsamad@taibahu.edu.sa

Received: 15 March 2014 / *Accepted:* 27 April 2014 / *Published:* 19 May 2014

The effect of H_2SO_4 acid concentration in range (1.0-12.0) M on corrosion resistance and ability of passive film formation on metallic glassy $Fe_{68.6}Ni_{28.2}Mn_{3.2}$ (at %) alloy have been studied using AC and DC techniques at 30°C. The experimental data obtained from this methods revealed that corrosion resistance increases at concentration higher than 6.0M. The alloy is spontaneously passivated with high passive current densities in all studied concentrations. Localized corrosion effects were observed at 12.0M. XPS analysis indicate the formation of NiS film on the alloy, which be responsible for the corrosion resistance of iron – base alloy. The fundamental thermodynamic functions were determined and used to glean important information about corrosion and passive characterization .

Keywords: Iron – base; Acid concentration; Amorphous alloy; Corrosion; EIS ; XPS.

1. INTRODUCTION

Corrosion behavior is an important variable towards the determination of the durability of the components. Metallic glasses have not always been an easy system to study but owing to their excellent mechanical properties[1-3] and resilience, chemically homogeneous single phase solid solution metallic alloys of metallic glasses alloys show a great potential for load-bearing orthopedic applications. This shows that they are superior in many aspects to alternative biomaterials such as polymers and ceramics[4,5].

Gu et al. [6] reveled that iron-based bulk metallic glasses (BMGs) are characterized by high fracture strengths and elastic module, with some exhibiting fracture strengths near 4 GPa, 2–3 times more than those of conventional high-strength steels.

During the last few decades, there has been considerable interest in the corrosion resistance of amorphous alloys. Aggressive acid media and temperature highly effected the corrosion behavior of the glassy alloys [7-12].

$Fe_{68.6}Ni_{28.2}Mn_{3.2}$ glassy alloy has not received many studies on its corrosion behavior in aggressive acid media. The goal of this work is to evaluate the corrosion behavior and passivity or pitting corrosion susceptible of $Fe_{68.6}Ni_{28.2}Mn_{3.2}$ alloy in H_2SO_4 acid solutions using different electrochemical techniques.

2. MARETRIALS AND METHODS

2.1 The specimens treatment

Alloy ingots with nominal composition $Fe_{68.6}Ni_{28.2}Mn_{3.2}$ (at %) (Vacoflex 2036, Vacuumschmelze GmbH & Co KG) with physical properties (density 8.1 g/cm^3, thermal extension 15.2× $10^{-6}K^{-1}$, specific electrical resistance 0.77μΩ m) was used. Electrochemical measurements were made using rectangular specimens of the bright face with a surface of 20mm × 10mm and thickness 0.25 mm. One test was conducted per sample. Before the test specimen was degreased in alcohol and rinsed several times with bi-distilled water and finally cleaned in an ultrasonic bath.

2.2 The electrolytic environments

Electrochemical characterization was performed in sulfuric acid solution in range (1.0-12.0)M. Each run was carried out in aerated stagnant solutions at the required temperature (±1˚C) using a water thermostat. Appropriate concentrations were prepared by dilution using bi-distilled water without further purification. The electrochemical cell consisted of the corrosion sample (working electrode), a saturated calomel reference electrode(SCE), and a platinum- wire counter electrode.

2.3 Methods

Electrochemical measurements were performed with ACM Gill AC at tested temperature. After immersion of the specimen, prior to the impedance measurement, a stabilization period of 20 min was found, which is sufficient to produced the steady- state potential (E_{ss}). Electrochemical impedance spectroscopy (EIS) measurements were performed at the frequency ranged from 30 kHz to 0.1 Hz with an amplitude of sinusoidal wave of 5 mV. Polarization measurements were performed at a scan rate of 2 mV/s, from -800 mV to 2000 mV .

To reveal the detailed micro-structural features of the investigated alloy under test condition, X-ray photo-electron spectra (XPS) from the alloy surface were measured, after the electrochemical test in 3.0M of test solution.

3. RESULTS AND DISCUSSION

3.1 Ac impedance studies

Nyquist plots for the $Fe_{68.6}Ni_{28.2}Mn_{3.2}$ alloy in H_2SO_4 acid solutions after 20 min immersion in the test solution at 30˚C are shown in Fig.1. The electrochemical impedance spectroscopy (EIS) helps to isolate the individual components describing the particular processes and properties of phases and interfaces, electrolyte resistance, charge transfer resistance (the fast process), double layer capacitance, adsorption and diffusion[13].

All experimental plots in Fig.1 have a depressed semicircular shape in the complex impedance plane, with the center under the real axis. This behavior is typical for solid metal electrodes that show frequency dispersion of the impedance data and has been attributed to roughness and other in homogeneities of the solid surface. In these cases the parallel network charge transfer resistance–double layer capacitance (R_{ct}–C_{dl}) is usually accepted as a poor approximation. When a non-ideal frequency response is present, it is commonly accepted to employ distributed circuit elements in an equivalent circuit. Constant phase element (CPE), which has a non-integer power depending on the frequency, is widely used as a model in place of a capacitor, to compensate the non-homogeneity in the system[14]. The impedance of a CPE is described by the expression:

$$Y_{CPE} = A^{-1}(j\omega)^{-n} \quad (1)$$

where A is a proportionality coefficient, ω the angular frequency (in rad s^{-1}), *j* is the imaginary number (j^2 = -1), ω is the phase angle of the CPE (in rad /s) and *n* has a meaning of a phase shift and can be used as a measure of the surface in homogeneity . For n=0, Z_{CPE} represents a resistance with R = A^{-1}, for n = 1 a capacitance with C= A, for n = 0.5 a Warburg element and for n =−1 an inductance with L=A^{-1} [15]. The smaller values of n, the higher the surface roughness. The HF capacitive loop, R_{ct} , CPE, can be attributed to the charge transfer presses. The charge transfer resistance (R_{ct}) (corrosion rate) values are calculated from the difference in impedance at lower and higher frequencies.

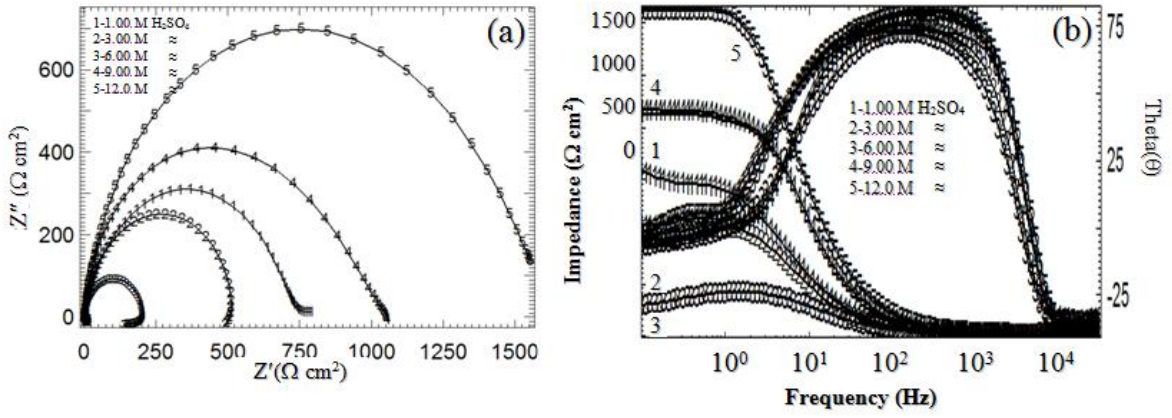

Figure 1. EIS plots for $Fe_{68.6}Ni_{28.2}Mn_{3.2}$ alloy in different concentrations of H_2SO_4 acid. Nyquist (a) and Bode (b).

Figure 1a shows a capacitive arc at high and intermediate frequencies (HF and MF) followed by inductive loop at low frequencies (LF), at the concentration of 6.0 M H_2SO_4 acid . The first capacitive arc corresponds to the combined effect of double layer capacitance and metal dissolution, and its diameter is related to the charge transfer resistance (R_{ct}) at the metal / solution interface. Evidently, the increase of concentration of acid decreased the diameter of the first capacitive arc until 6.0M, therefore, dissolution rates for the alloy are increased. Critical behavior is observed at 9.0 and 12M of acid where the alloy resistance increases as the acid concentration increases. Nevertheless, R_{ct} values were representative of the dissolution of not only Fe (the major and active alloying element) but also other alloying elements [15,16]. The inductive behavior observed at low frequencies for the alloy at 6.0M H_2SO_4 acid, attributed to the formation of Fe(I) and Fe (II) adsorbed intermediate species in the active region for Fe in the studied solutions [17] .

As Nyquist diagrams, lower polarization resistance (R_P) value recorded at 6.0 M H_2SO_4 associated with shorter relaxation times was show in Bode- plot, Fig.1b. The phase angle (Θ_{max}) values approach 85° suggesting that the electrochemical process occurring at high frequency favors the charge transfer process.

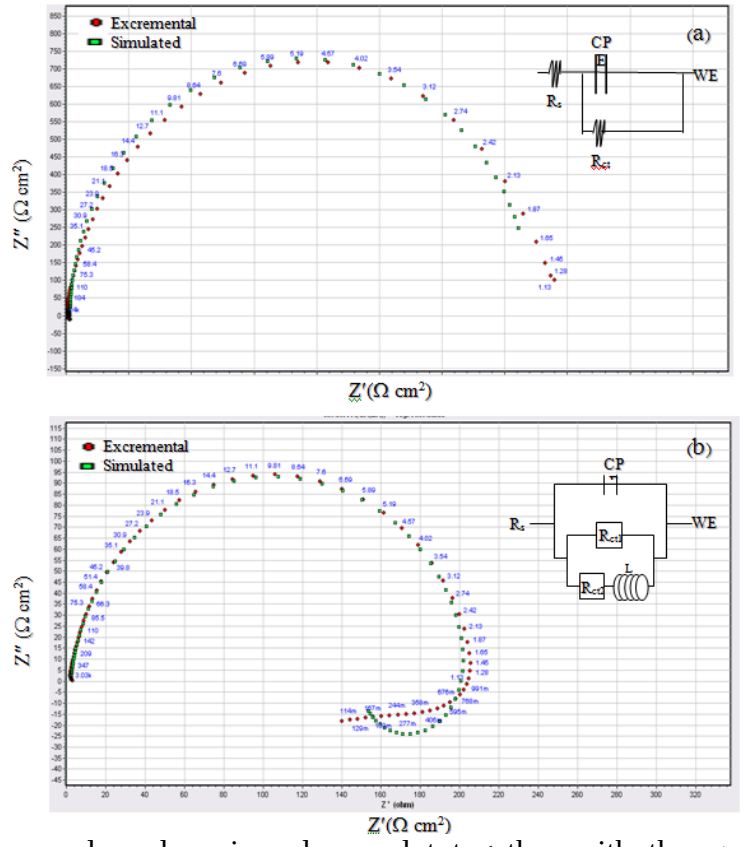

Figure 2. (a) Simple complex plane impedance plot, together with the equivalent circuit. $R_s(R_{ct}Q)$. R_s; ohmic resistance of the electrolyte, R_{ct}; charge transfer resistance and Q(CPE); double layer capacity. (b) Complex plane impedance plot, together with the equivalent circuit models fitting for spectra consist inductive loop. Is R_s ($R_{ct1}Q(LR_{ct2})$). R_s; ohmic resistance of the electrolyte, R_{ct1}; charge transfer resistance, and R_{ct2}; resistance through the pit and L; the inductive contribution.

The best fitted parameter results for $Fe_{68.6}Ni_{28.2}Mn_{3.2}$ alloy corrosion, using *ZSimDemo* impedance modeling software are presented in Table 1. Figs. 2a and 2b observed that the fitted data follow a similar pattern as the original results along the diagrams, with a percentage error smaller than 4% in all cases (the quality of fitting to the equivalent circuit (EC) was judged firstly by the Chi- square (χ^2) values and secondly by the error distribution versus frequency, comparing experimental with simulated data). The electrical equivalent circuit employed to analyze the impedance spectra with one capacitive loop and in presence of inductive behavior also show in Figs. 2a and 2b, respectively.

Table 1. Electrochemical kinetic parameters and corrosion rate obtained by EIS technique for $Fe_{68.6}Ni_{28.2}Mn_{3.2}$ alloy in naturally aerated H_2SO_4 solutions at 30°C.

C_{HCl} (M)	R_{ct} (Ωcm^2)	CPE (Q) ($\mu F/cm^2$)	n	χ^2	Corrosion rate mm/y
1.00	744	74.22	0.88	0.16×10^{-2}	0.38
3.00	541	75.76	0.92	0.20×10^{-2}	0.54
6.00	207	93.65	0.93	0.30×10^{-2}	1.39
9.00	1029	24.07	0.96	0.24×10^{-2}	0.28
12.0	1535	22.87	0.94	0.26×10^{-2}	0.18

It is obvious from Table 1 that the value of the charge transfer resistance, R_{ct} decrease with the concentration increase and reached a minimum value of 207 Ωcm^2 at 6.0 M (decrease in R_{ct} values about 72.2% and Q increase about 69%). Farther increase in acid concentration leads to an increases the diameter of capacitive arc (increase in R_{ct} values and decrease Q values).

This phenomenon explained by the role of relative humidity on the corrosion rate. At high humidity and low H_2SO_4 acid concentration, the corrosion rate (deposition rate) is sufficiently high to prevent the buildup of any protective layer. Low humidity allow the protective layer form.

3.2 DC electrochemical results

In order to clear the susceptible of $Fe_{68.6}Ni_{28.2}Mn_{3.2}$ alloy for passivition or pitting corrosion in H_2SO_4 acid, the cyclic potentiodynamic polarization used. After impedance run, the potential was sweep from cathodic to anodic directions and then the reverse, noble- active, polarization is essential to study the localized corrosion or breakdown of passivity.

Corrosion current densities (I_{corr}) were calculated by extrapolating the Tafel lines to corrosion potential (E_{corr}). Passivation parameters: critical passivation current density (I_{cc}), critical passivation potential (E_{cc}), passivation potential (E_{pass}), passivation current density (I_{pass}) were determined from the potentiodynamic polarization curve and summaries in Table 2.

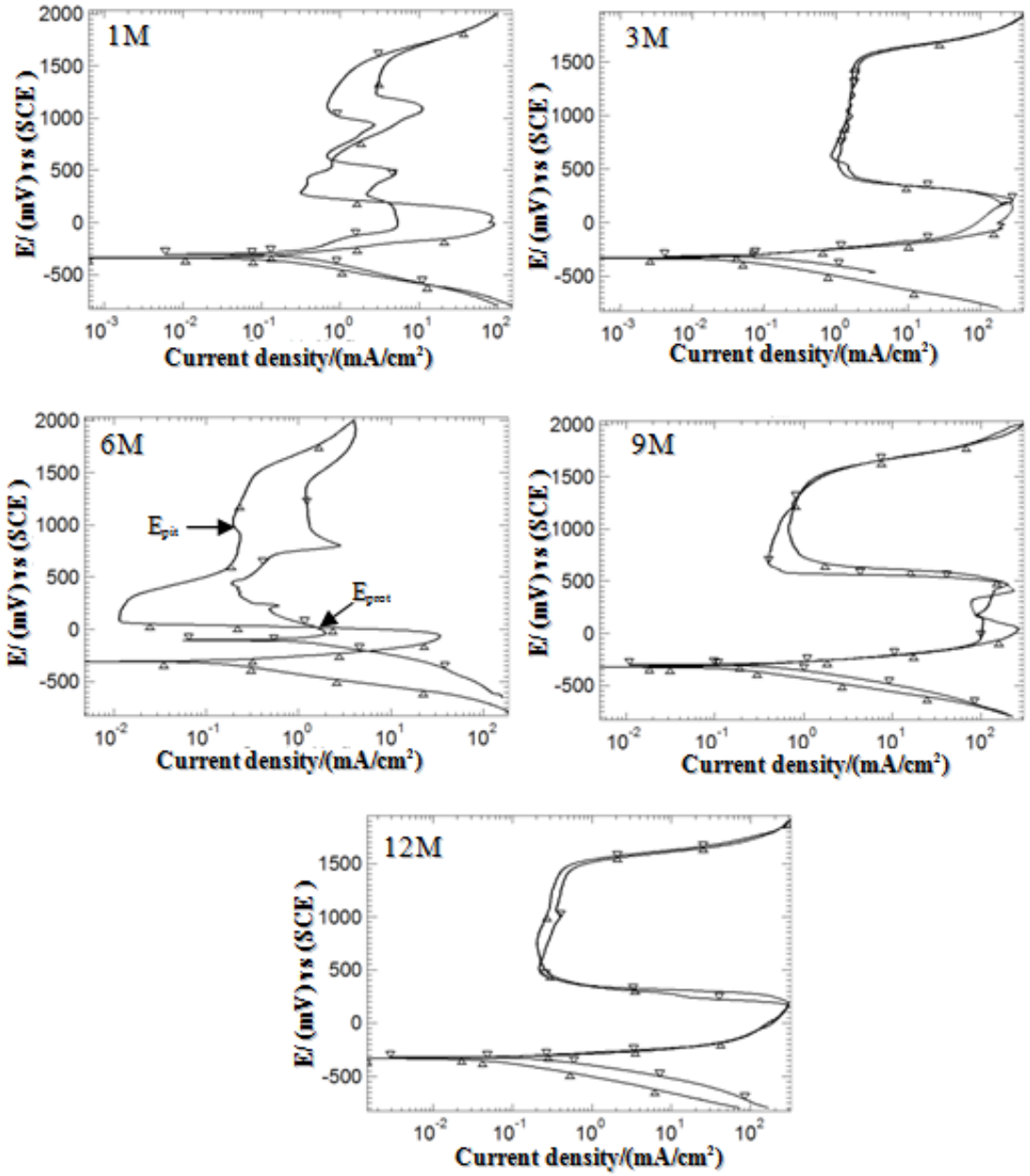

Figure 3. Tafel plots for $Fe_{68.6}Ni_{28.2}Mn_{3.2}$ alloy after the immersion in different concentrations of H_2SO_4 at 30˚C.

Figure 3, shows active - passive behavior on both forward and reveres scan in all examined acid concentrations in H_2SO_4 acid solutions. Cathodic polarization curves are slightly shifted towards higher current densities. Evolution of hydrogen gas was observed during the cathodic reaction in each case . Polarization curves indicated that the values of corrosion rate (I_{corr}) increase with the increase of the acid concentrations up to 6.0M . At this concentration, a big positive hysteresis presence which is typical of the localize (pitting or crevice) corrosion behavior of metals. A material's susceptibility to pitting or localized corrosion can be evaluated by the hysteresis area observed in its polarization curve obtained in an aqueous solution containing aggressive ions.

Table 2. Electrochemical parameters of polarization for $Fe_{68.6}Ni_{28.2}Mn_{3.2}$ alloy in naturally aerated H_2SO_4 solutions at 30°C.

H_2SO_4 *con.(M)*	$-E_{corr}$ *mV/SCE*	$I_{corr} \times 10^2$ mA/cm^2	E_{cp} mV/SCE	E_{pass} mV/SCE	I_{cc} mA/cm^2	I_{pass} mA/cm^2	E_b mV/SCE
01.0	**343**	**3.50**	**47**	**282**	**90**	**2.47**	**1519**
03.0	**334**	**4.98**	**148**	**455**	**320**	**1.71**	**1490**
06.0	**315**	**12.8**	**-65**	**85**	**33**	**0.22**	**1428**
09.0	**327**	**2.53**	**399**	**797**	**185**	**0.75**	**1422**
12.0	**329**	**1.64**	**187**	**486**	**303**	**0.27**	**1417**

This area can be considered as being proportional to the difference between the critical pitting potential and the protection potential (the susceptible pitting factor) $\Delta E = (E_{pit} - E_{prot})$.The bigger this potential difference, the smaller the material's pitting corrosion resistance[18]. The $(E_{pit} - E_{prot})$ value was found to be 973mV, which reflex the high localized corrosion susceptibility of $Fe_{68.6}Ni_{28.2}Mn_{3.2}$ alloy at 6.0M H_2SO_4 acid.

At higher concentrations the effect of opposite process controls the reaction. The latter process make the oxide layer more thicker and decrease the (I_{corr}) values in this condition, that means the healing of the oxide film under low humidity conditions resulting in the formation of compact barrier oxide film.

The increase in I_{corr} associated with markedly increase in I_{cc} and E_{cp} in the positive direction indicating delay in protective layer formation.

The high values of both the passivation tendency, I_{cc} and degree of passivation, I_{Pass} in forward scan can be attributed to a non adhering porous layer. This hypothesis may be confirmed because at the end of polarization test the sample surface looked gray and the solution had returned yellow. The reveres scan also show less effective in alloy protection.

3.3 X- Ray photo – electron spectroscopy (XPS) (XPS)

The corrosion behavior of $Fe_{68.6}Ni_{28.2}Mn_{3.2}$ alloy was further examined by XPS analysis of the surface film in 3.0M experiment after impedance and polarization tests.

The peak binding energies of the Ni $2p_{3/2}$ electron in Fig. 4 were about 852.8 and 852.9 - 853.1 eV estimated for both before (as-resaved) treatment and after treatment (after the experiment) at different scattering times in H_2SO_4 acid. Fe $2p_{3/2}$ electron was observed at 710.8 eV which means that Fe is found as $FeCl_3$ which is also soluble [19]. The peak binding energy of S $2p_{3/2}$ electron was observed at 162.3 indicated the presence of NiS on the alloys surfaces

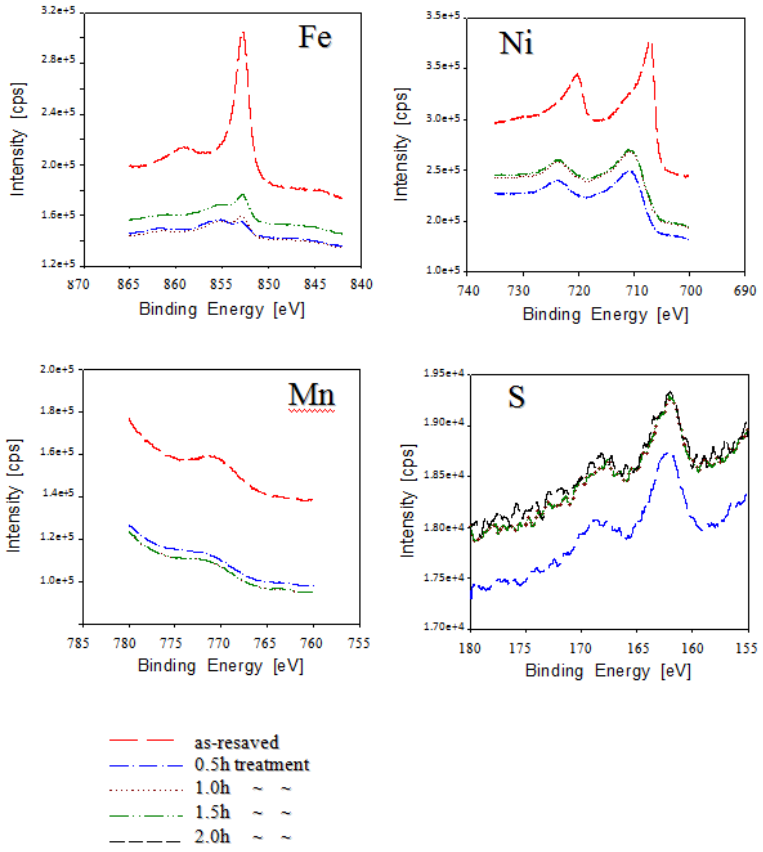

Figure 4. X $2p_{3/2}$ photo-electron spectra obtained for $Fe_{68.6}Ni_{28.2}Mn_{3.2}$ alloy before and after the experiment in 3.0M H_2SO_4 acid solutions.

3.4 Thermodynamic parameters

There have been limited publications on the corrosion behavior on metallic glasses alloys at different temperatures have been done. Low aggressivity in the studied temperature range led to chose 3.0 M of acids to study of the electrochemical behavior of $Fe_{68.6}Ni_{28.2}Mn_{3.2}$ glassy alloys at different temperatures before the specimen destroyed specially at high temperature.

Figs.5a,5b show the influence of temperature on pitting and general corrosion behavior of $Fe_{68.6}Ni_{28.2}Mn_{3.2}$ glassy alloy in 3.0M acid solutions at various temperatures in the domain (30-60)ºC by Impedance diagrams. A sudden drop appeared in H_2SO_4 acid. solutions at temperatures higher than 30ºC. The results in Table 3 indicates that the drop occurs in hot solutions and in 60°C gives the worst resistivity (92.77% lower than at 30°C). The increase in Q values can be correlated to the increase in the corroded area of the alloy surface.

The acceleration of anodic process occurs more quickly at higher temperatures and this reflex the inductive loop at the end of the Nyquist plot at temperatures higher than 30ºC which indicate that the Faradic process takes place (localized attack) on the iron base alloy. Values of corrosion rate (mm/y) increase and reach an unacceptable values of about 7.279 mm/y at 60ºC in H_2SO_4 acid. The single peaks can be clearly observed in Bode – phase plots which become narrow as bulk acid temperature increase, (shorter time constants, fast reaction). This

phenomenon can be explained by the fact that the time lag between the process of formation and dissolution of passive film molecules over metal surface becomes shorter with increase in temperature. The phase angle Θ_{max} of single Bode peak decreases gradually at alloy / solution interface from 80 to 60° indicating that electrochemical process occurring at high frequency doesn't favors the passive film formation.

Table 3. Electrochemical parameters of impedance measurements for $Fe_{68.6}Ni_{28.2}Mn_{3.2}$ alloy in different temperatures H_2SO_4 solutions.

Temperature °C	R_{ct} (Ωcm^2)	CPE (Q) ($\mu F/cm^2$)	n	χ^2	Corrosion rate mm/y
30	541	75.76	0.92	0.16×10^{-2}	0.54
40	167	93.17	0.93	0.19×10^{-2}	1.55
50	73.8	93.86	0.94	0.24×10^{-2}	3.85
60	39.1	118.60	0.90	0.22×10^{-2}	7.28

If n is also accepted to be measure of the surface inhomogeneity, then its decrease should be connected with certain increase in heterogeneity resulting from surface metal roughening. The latter may be caused by enhanced dissolution of metal, which takes place at high temperatures during exposure to the solution.

Figure 5c reveal that the cathodic polarization curves were linear and shifted towards higher current density region with increase in the test solution temperature association by huge hydrogen evolution. Rising of the temperature is associated with the increase in the corrosion current density ($I_{corr.}$). The highest current oscillations were observed at 60°C with a maximum amplitude of $6.68x10^{-1}$ mA/cm^2, (92.54 higher than at 30°C), this behavior may due to pitting attack by S^{-2} produced through SO_4^{-2} reduction [20] , as shown in impedance plots, which reveal good agreement between the polarization and impedance measurements.

Active - passive and transpassive behavior was observed for $Fe_{68.6}Ni_{28.2}Mn_{3.2}$ alloy except at 60ºC. The nature of the curves is similar. This indicate that the iron base alloy is spontaneously passivated at employ temperatures in range (30-50ºC). Increasing temperature was apt to increase the anodic current density but corrosion potential does not show a regular trend. It was marked by high active - passive peaks (high values of I_{cc}) and sharp passivity region is also not obtained in most of the cases. It appears that temperature destabilizes the passivity and highly unstable passive film formed on the alloy surface at high temperatures. High values of I_{cc} may be attributed to a further increase in the uncovered area resulting in follow a very high current density before passive film formation. The absence of anodic passivation oxide layer at 60ºC cause direct diffusion of the acid to the alloy /solution interface leading to a quick dissolution of alloy component.

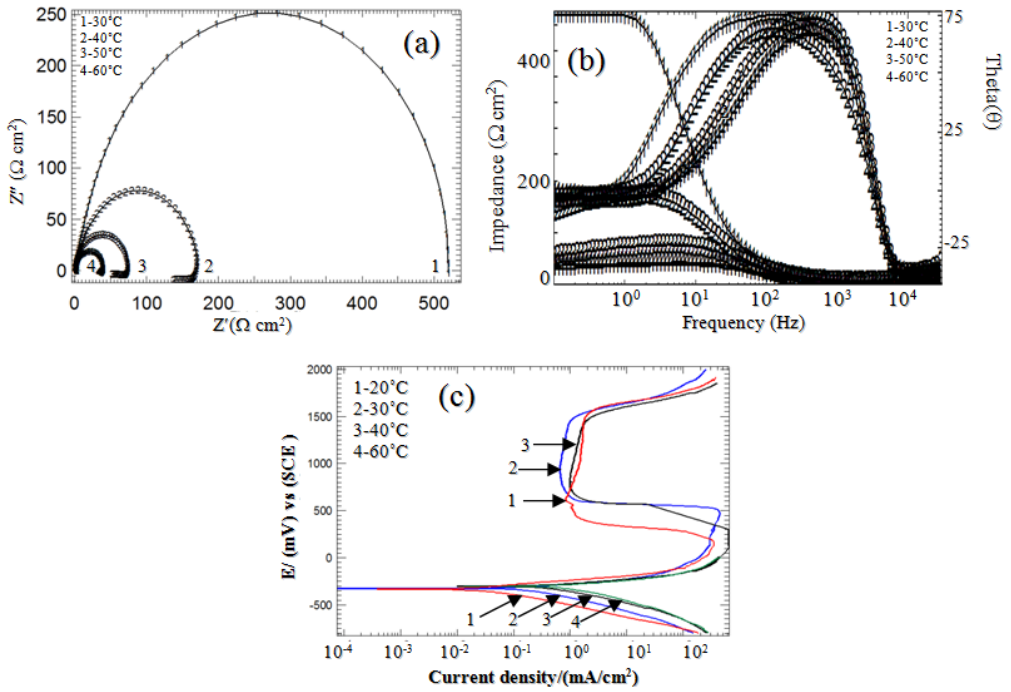

Figure 5. (a) Nyquist , (b) Bode Impedance and (c) polarization diagrams for $Fe_{68.6}Ni_{28.2}Mn_{3.2}$ alloy in different temperatures of H_2SO_4 acid .

Evolution of oxygen on the alloy surface was observed in the transpassive region. The sharp increase in the current density in this region was attributed to the dissolution or breakdown of NiS passive film which occur in same mechanism at all temperatures.

After polarization experiment, the specimens became grey and the solution turned colorless to green yellowish. The color became dark with the temperature increase. In highest temperature the passive film will be removed and the alloy directly attacked by S^{-2} ion which may cause crevice corrosion so the specimens fall in the test solution.

In all cases, we note an increase of corrosion current density and decrease in charge resistance with increasing temperature indicating the activation the corrosion process.

The values of activation energy (ΔE^*_{app}) for the dissolution of glassy $Fe_{68.6}Ni_{28.2}Mn_{3.2}$ alloy in 3.0M Sulfuric acid was calculated from the Arrhenius type plot according to the following equation:

$$i_{corr.} = A\exp\left(-\frac{\Delta E^*_{app}}{RT}\right) \qquad (2)$$

$$1/R_{ct} = A\exp\left(-\frac{\Delta E^*_{app}}{RT}\right) \qquad (3)$$

where R is the gas constant, A is Arrhenius constant and T is the absolute temperature. Activation energy was calculated from the slope of log $I_{corr.}$ or log $1/R_{ct}$ as a function of (1/T) plots with using least square method (LSM) by *Sigma Plot* Program, Fig.6.

Table 4. The values of activation parameters ΔE_a, ΔH^* and ΔS^* for $Fe_{68.6}Ni_{28.2}Mn_{3.2}$ alloy corrosion in 3.0 M H_2SO_4 .

Impedance				Polarization			
ΔE^*_{app} ($kJmol^{-1}$)	ΔH^* ($kJmol^{-1}$)	ΔS^* ($Jmol^{-1}K^{-1}$)	r^2	ΔE^*_{app} ($kJmol^{-1}$)	ΔH^* ($kJmol^{-1}$)	ΔS^* ($Jmol^{-1}K^{-1}$)	r^2
71.99	69.35	-67	0.983	71.67	68.95	-41	0.983

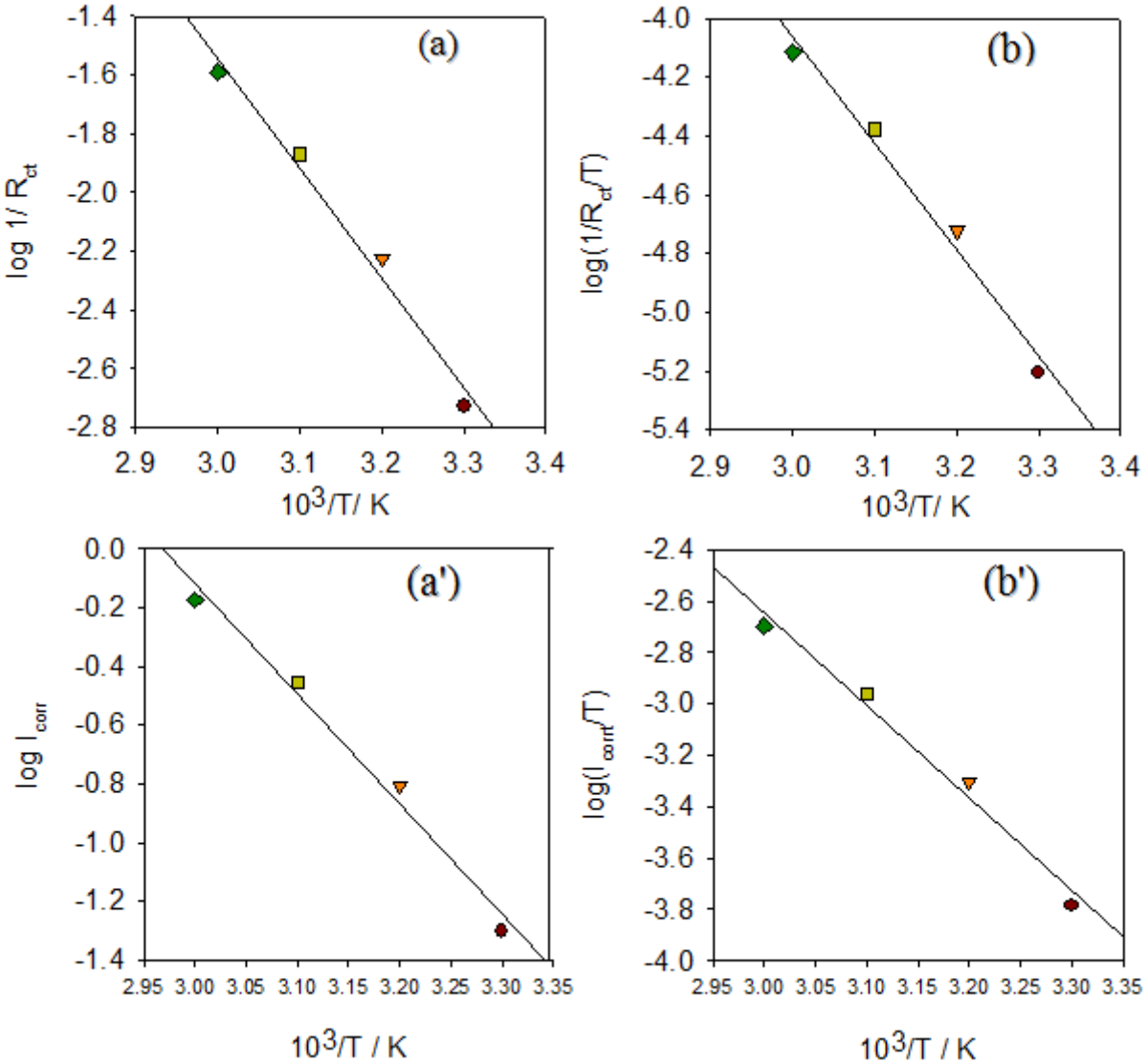

Figure 6. (a,a') Arrhenius and (b,b') transition state plots for $Fe_{68.6}Ni_{28.2}Mn_{3.2}$ alloy before and after the experiment in 3.0M H_2SO_4 acid solution.

According to data in Table 4, low value of ΔS* (negative value) reflect the most order corrosion reaction, that mean the system close to equilibrium and the corrosion reaction take place. But it value is higher (less negative) than that determined in Hydrochloric acid solution (-192

$Jmol^{-1}K^{-1}$) [20] which. The low values of ΔS* reflect the presence of protective layer on $Fe_{68.6}Ni_{28.2}Mn_{3.2}$ alloy [21]. The positive signs of ΔH* reflect the endothermic nature of the glassy alloy dissolution process.

Apparent activation energy (ΔE^*_{app}) of hydrogen evolution reaction for 3.0M Sulfuric acid. is 71.99 $kJmol^{-1}$ which is higher than (ΔE^*_{app}) of same alloy in 3.0M Hydrochloric acid (24.96 $kJmol^{-1}$) [21]. This reveal that Sulfuric acid is the lower aggressive media for the glassy $Fe_{68.6}Ni_{28.2}Mn_{3.2}$, where Hydrochloric acid is the aggressive one. This means that the physical barrier (passive film) can probably affect the nature of the corrosion process.

Values of enthalpy ΔH* and entropy ΔS* for the corrosion of glassy alloy were calculated from the transition - state equation:

$$\left(\frac{I_{corr.}}{T}\right)=\left[\left(\frac{R}{Nh}\right)\exp\left(\frac{\Delta S^*}{R}\right)\right]\exp\left(-\frac{\Delta H^*}{RT}\right) \quad (4)$$

$$\left(\frac{1/R_{ct}}{T}\right)=\left[\left(\frac{R}{Nh}\right)\exp\left(\frac{\Delta S^*}{R}\right)\right]\exp\left(-\frac{\Delta H^*}{RT}\right) \quad (5)$$

where *h* is Plank's constant, *N* is Avogadro's number. Fig.6 show a plot of log (I_{corr} / T) or log ($1/R_{ct}$ / T) against 1/T gave straight line of slope (-ΔH*/2.303R) and the intercept is (log (R / *Nh*) + ΔS* / 2.303R) from which the values of ΔH* and ΔS* were deduced. The calculated thermodynamic parameters with standard deviation ,r^2, about 0.98 are given in Table 3.

4. CONCLUSIONS

The main conclusions drawn from the study of $Fe_{68.6}Ni_{28.2}Mn_{3.2}$ glassy alloy in H_2SO_4 acid solutions are:

- The process on the interface mild iron base/(1.0-9.0) H_2SO_4 acid solutions are described by a simple equivalent circuit including a charge transfer resistance, R_{ct}, a parallel double-layer capacitance which distributed and modeled by a CPE element and ohmic resistance, R_s at 30°C.
- The corrosiveness of H_2SO_4 acid solutions increase up to 6.0M and after this critical concentration the passivation process control.
- At 30°C, inductive behavior (susceptibility for localized corrosion) only shows at 12.0M H_2SO_4 acid .
- According to EIS and polarization measurements, localized corrosion starting observing at 40°C .
- At temperature in the range of 30-60°C, apparent activation energy ΔE^*_{app}, enthalpy ΔH* and entropy ΔS* for the corrosion of glassy alloy were calculated and discussed.

ACKNOWLEDGEMENT

The author would like to acknowledge professor Sanaa T. Arab and Dr. Hamad A.Al-Turaif, King Abdulaziz University. Also wish to express their gratitude to Dr.Hartmann Thomas from Vacuumschmelze company for supplying the iron base alloy of this research .

References

1. X. Li, C.Qin, H. Kato, A. Makino, A. Inoue, A. , *J. Alloys Compd.*, 509(29) (2011) 7688-7691.
2. K. Takenaka, N. Togashi, N. Nishiyama, A.Inoue, *J. Non-Cryst. Solids*, 356(31-32) (2010) 1542- 1545.
3. K. A. Lee, K. A. , Y. C. Kim , J. H. Kim, Ch. S. Lee,J.Namkung, M.ChulKim, *Mater. Sci. & Eng.*, A449-451(2007) 181-184.
4. J.Namkung, , M. C. Kim, C. G. Park, *Mater. Sci. & Eng.*, 449–451 (2007) 430-434.
5. J.Basu, S. Ranganathan, *Sadhana*, 28 (2003) 783–798.
6. X. J. Gu, , S. J. Poon, G. J. Shiflet, *J. Mater. Res.*, 22(2007) 344-351.
7. B. P. Zhang, H. Habazaki, A. Kawashima, K. Asami, K. Hashimoto, *Corros. Sci.*, 33(10) (1998) 1519-1528.
8. A . Kawashima , H. Habazaki, K. Hashimoto, *Materi. Sci. & Eng.: A* , 304-306 (31) (2001) 753-757.
9. S. T. Arab, K. M .Emran, *Int. J. Appl. Chem.*, 3(1) (2007) 69–84 .
10. S.T. Arab, K. M. Emran, *Phy. Chem. News*, 50(2009) 131-139.
11. J. Paillier, Ch. Mickel, P. F. Gostin, A.Gebert , *Mater. Charact.*, 61(10) (2010) 1000-1008.
12. S. Liu, L.Huang, Sh. Pang, *Int. J. Miner. Metall. Mater.*, 19(2) (2012)146-150.
13. M. M. Hukovic, S.Omanvic, *J. Electroanal. Chem.*, 455(1-2) (1998)181-189.
14. J. R. Macdonald, Impedance Spectroscopy—Emphasizing Solid Materials and Systems, A Wiley-Interscience Publication 1987.
15. A. Pardo, M. C.,Merino, A. E. Coy, F. Viejo, R. Arrabal, E. Matykina, *Corros. Sci.*, 50(3) (2008) 780- 794.
16. S. T. Arab, K. M. Emran, *Mater. Lett*, 63(6-7) (2008) 1022-1032.
17. M. Keddam , O. R. Mattos, H. Takenouti , *Electrochim. Acta*, 31(9) (1986) 1147-1158.
18. E. Kikuti, R. Conrrado, N. Bocchi, S.R. Biaggio, R.C. Rocha– Filho, *J. Braz. Chem. Soc.*, 15(4) (2004) 472-480.
19. J. M. Le Canut, S. Maximovitch, F. Dalard, *J. Nucl. Mater.*, 334(1) (2004) 13-27.
20. K. M. Emran, " Effects of concentration and temperature on the corrosion properties of the Fe–Ni–Mn alloy in HCl solutions ", *Res. Chem. Intermed.* In Press, On line (2013),
21. J. Marsh, " Advanced Organic Chemistry", third ed., Wiley Eastern, New Delhi 1988.